OXYGEN ISOTOPIC COMPOSITIONS OF INDIVIDUAL MINERALS FROM FUN CAIS. A. N. Krot[1*], K. Nagashima[1], I. D. Hutcheon[2], A. M. Davis[3], K. Thrane[4], M. Bizzarro[4], G. R. Huss[1], D. A. Papanastassiou[5,6], and G. J. Wasserburg[6]. [1]HIGP/SOEST, Univ. of Hawai'i at Manoa, Honolulu, HI, USA. *sasha@higp.hawaii.edu. [2]Lawrence Livermore National Lab., Livermore, CA, USA. [3]Dept. of Geophysical Sciences & Enrico Fermi Institute, Univ. of Chicago, Chicago, IL, USA. [4]Geological Institute, Copenhagen, Denmark. [5]Jet Propulsion Lab, Pasadena, CA, USA. [6]The Lunatic Asylum, Div. of Geological & Planetary Sciences, CalTech, Pasadena, CA, USA.

Introduction: Calcium-aluminum-rich inclusions (CAIs) with Fractionation and Unidentified Nuclear isotope anomalies (FUN CAIs [1-3]) are rare objects characterized by large mass-dependent fractionation effects in Mg, Si and O, relatively large non-linear anomalies in several elements (e.g., Ca, Ti, Si), and low inferred abundance of ^{26}Al. On a three-isotope oxygen diagram, compositions of whole-rock and isolated minerals or density fractions from several FUN CAIs plot to the right of the Allende CAI line and define lines that converge on a single composition [4–7]. Based on these data and ^{16}O-rich compositions ($\Delta^{17}O \sim -20‰$) of normal CAIs, Clayton and Mayeda [6] suggested that FUN CAIs evolved from ^{16}O-rich melts by mass fractionation prior to crystallization followed by isotopic exchange with an ^{16}O-poor ($\Delta^{17}O > -5‰$) gaseous reservoir. The only *in situ* measurements of O-isotopic compositions of individual minerals from the forsterite-bearing FUN CAI Vigarano *1623-5* [8] are generally consistent with this hypothesis, but indicate some isotopic fractionation during crystallization of the CAI melt as well. Here we report *in situ* O-isotope measurements of individual minerals from previously identified and mineralogically characterized Allende FUN CAIs *C1* [4,5], *EK1-4-1* [6], *CG-14* [7], *BG82 B7F6* [9], *BG82 DH8* [9], and Allende F CAI *TE* [10–12] measured with the University of Hawai'i Cameca ims-1280 ion microprobe. The mineralogy, petrography, Mg- and O-isotopic compositions of a newly identified wollastonite-bearing Type B FUN CAI from NWA 779 (CV3), *KT-1*, are reported in [13].

Samples and Analytical Techniques: Polished thin and thick sections, fragments and isolated grains from the CAIs were studied using optical and scanning electron microscopy (SEM), electron probe microanalysis (EPMA) and ion microprobe (SIMS). All samples were mapped in Ca, Al, Mg, Ti, Na, Si, and Cl Kα X-rays with a Cameca SX-50 electron microprobe and studied in the backscattered electron mode with the JEOL 5900LV SEM/EDS. Oxygen isotopic compositions were measured with the University of Hawai'i Cameca ims-1280 ion microprobe in multicollection mode. A focused Cs^+ primary beam of 1.8 nA was used to presputter regions of 25×25 μm^2. The raster size was then reduced and oxygen isotopes were measured from the ~10×10 μm^2 central region. The ^{16}O and ^{18}O ion beams were measured at Mass Resolving Power (MRP) ~2000 using Faraday cups of multicollector; ^{17}O was measured using electron multiplier (EM) of monocollector at MRP ~5500. Instrumental mass fractionation (IMF) effects were corrected by analyzing San Carlos olivine, Burma spinel, Miyakejima anorthite and Cr-augite. Melilite and wollastonite compositions for which standards were lacking were corrected by assuming their IMF are similar to those of San Carlos olivine and augite, respectively. 2σ uncertainties ~1‰ in $\delta^{17}O$ and ~1.5‰ in $\delta^{18}O$ were estimated from overall standard data obtained during all sessions. Most samples were measured in more than two sessions. There are no systematic differences between the sessions or sample mounts.

Oxygen isotopic compositions: *C1:* Several spinel-fassaite-anorthite fragments and isolated grains were measured. Data for spinel and fassaite plot along a mass-dependent fractionation line that intersects the Allende CAI line at $\delta^{17}O = -49‰$, $\delta^{18}O = -48‰$ ($\Delta^{17}O \sim -24‰$). This array (hereafter, the FUN FL) is indistinguishable from the fractionation line defined by spinel, fassaite and forsterite from the FUN CAI 1623-5 [8]. Spinel grains are generally less fractionated than fassaite (Fig. 1a). Anorthite and melilite are ^{16}O-depleted and plot near the TFL ($\Delta^{17}O \sim -3‰$).

EK1-4-1: Isolated grains of spinel and fassaite on bullets and small (<100 μm) spinel-fassaite±melilite fragments on a glass section were measured. The data for spinel and fassaite plot along the FUN FL (Fig. 1b). Melilite is ^{16}O-depleted and plots near the TFL ($\Delta^{17}O \sim -3‰$).

BG82 DH8: The CAI consists of several irregularly-shaped spinel-fassaite-rich objects; melilite and anorthite are minor and extensively replaced by sodalite, nepheline and ferrous olivine. The outer portion of the CAI contains abundant intergrowths of lath-shaped hibonite and spinel. Several coarse (~50 μm), euhedral Ca-rich forsterite grains intergrown with fassaite are observed near the edge. They may belong a forsterite-fassaite-rich inclusion that forms a compound object with DH8. Data for spinel, forsterite and most fassaites plot along the FUN FL (Fig. 1c). Anorthite, melilite and two spots in fassaite are ^{16}O-depleted and define an exchange line similar to that reported for fassaite and melilite in KT-1 [13] (Fig. 1d).

BG82 B7F6: The CAI consists of abundant spinel and minor interstitial fassaite. Several aggregates of coarse (~50 μm) euhedral forsterite grains surrounded by secondary nepheline, sodalite and ferrous olivine occur near the edge of the CAI. They may belong a forsterite-fassaite-rich inclusion that forms a compound object with B7F6. Data for spinel, forsterite and fassaite plot along the C1 fractionation line (Fig. 1e).

CG-14: A fragment containing the spinel-fassaite and forsterite-fassaite-rich lithologies (Fig. 4 in [7]) was measured. Data for spinel, forsterite and fassaite plot along the FUN FL; spinel and fassaite are the least and the most fractionated minerals, respectively (Fig. 1f). Melilite is ^{16}O-depleted ($\Delta^{17}O \sim -3‰$). Whole-rock data reported by [7] plot near the line connecting fassaite analyses and melilite.

TE: Several ~100 μm fragments from the forsterite-fassaite lithology [10-12], were measured. Data for spinel, fassaite and forsterite plot along mass-dependent fractionation line with $\Delta^{17}O \sim -16‰$, different from the FUN FL. Most analyses cluster around whole-rock value reported by [7] ($\delta^{17}O \sim -6‰$, $\delta^{18}O \sim -20‰$); several forsterite grains in two fragments with abundant secondary phases are more fractionated ($\delta^{17}O$ and $\delta^{18}O$ up to −15‰ and 3‰, respectively).

Discussion: Oxygen isotopic compositions of spinel, fassaite and forsterite from the six FUN CAIs measured indicate progressive evaporation and mass fractionation during crystallization of the CAI melts having initially similar O-isotopic composition at $\delta^{17}O = -49‰$, $\delta^{18}O = -48‰$ for the intersection point with the CAI line [14,15]. We note that O-isotopic compositions of spinel, forsterite and fassaite from several forsterite-bearing CAIs plot along the same fractionation line, but are much less fractionated [16]. The observed differences in the degree of fractionation between normal and FUN CAIs could be due to kinetics and conditions of evaporation. We suggest that for normal CAIs, evaporation resulted from transient heating events at high ambient pressure when fast evaporation, back reactions and exchange with the gas minimized the mass fractionation [15,17]. In contrast, FUN CAIs evaporated more slowly, under low total pressure, under conditions that approximate Rayleigh distillation, possibly during initial infall [15,18,19]. As there was no significant back reaction or ex-

change with the gas, isotopic anomalies in the precursors were not diluted by isotopically normal material. Subsequently, at least two FUN CAIs, DH8 and KT-1, experienced incomplete melting and isotopic exchange of fassaite, melilite and anorthite in an ^{16}O-depleted ($\Delta^{17}O \sim -3‰$) nebular reservoir. In other FUN CAIs, the lack of evidence for remelting and isotopic exchange in fassaite and extensive *in situ* alteration of these CAIs (presence of hedenbergite-andradite-wollastonite rims around altered portions of CAIs and veins crosscutting them) may indicate the ^{16}O-poor compositions of melilite and anorthite in these CAIs reflect isotopic exchange during fluid-assisted thermal metamorphism on the CV asteroid [20].

Only few FUN CAIs show excesses of ^{26}Mg (^{26}Mg*) due to decay of ^{26}Al: C1 [21], HAL [22], and 1623-5 [23]; the inferred ^{26}Al/^{27}Al ratio is $<<5\times10^{-5}$. No ^{26}Mg* was detected in other FUN CAIs [9,13]. The canonical ^{26}Al/^{27}Al ratio was inferred for rim hibonites around F CAI TE [12]. The low abundance of ^{26}Al in FUN CAIs could either be due to their very late formation or due to the lack of the canonical ^{26}Al inventory in their precursors. If the absence of ^{26}Al is due to late formation, then there is a serious problem in explaining the anomalies attributed to nucleosynthetic effects as well as ^{16}O-rich compositions of FUN CAIs. This would require that they formed in a region that partially preserved incompletely mixed presolar components which had no ^{26}Al, implying gross heterogeneity in the distribution of ^{26}Al in the late solar nebula. It is also inconsistent with the inferred evolution of O-isotopic composition of the solar nebula [24]. Alternatively, FUN CAIs could have formed by thermal processing of dust balls that aggregated early and largely avoided late-injected, freshly synthesized, ^{26}Al-enriched dust [19]. We note that the observed UN isotopic effects in many elements for FUN CAIs may be due to non-linear isotopic effects produced by UV irradition as has been observed experimentally and proposed theoretically [25-27]. This effect would remove the apparent necessity that the FUN CAIs be "old". In this case, the non-linear affects are present in the FUN CAIs because they represent an integral part of the evaporation process that is not erased by back reactions. We note, however, that if such non-nucleosynthetic processes are applicable in the early solar nebula and during CAI formation, a higher frequency of FUN inclusions is expected.

References: [1] Wasserburg et al. (1977) *GRL, 4*, 299. [2] Lee et al. (1980) *GRL, 7*, 493. [3] Lee et al. (1979) *Ap. J. 228*, L93. [4] Clayton et al. (1977) *EPSL, 34*, 209. [5] Gray et al. (1973) *Icarus, 20*, 213. [6] Clayton & Mayeda (1977) *GRL, 4*, 295. [7] Clayton et al. (1984) *GCA, 48*, 535. [8] Davis et al. (2000) *MAPS, 35*, A47. [9] Brigham (1990) *PhD Thesis, CalTech*. [10] Dominik et al. (1978) *PLPSC, 9*, 1249. [11] El Goresy et al. (1989) *Meteoritics, 24*, 263. [12] El Goresy et al. (1991) *LPS*, 22, 345. [13] Thrane et al. (2008) this vol. [14] Scott & Krot (2001) *MAPS, 36*, 1307. [15] Wood (1981) *EPSL, 56*, 32. [16] MacPherson et al. (2008) this vol. [17] Richter et al. (2007) *GCA, 71*, 5544. [18] Wood (2004) *GCA, 68*, 4007. [19] Wood (1998) *ApJ, 503*, L103. [20] Nagashima et al. (2007) *LPS, 38*, #2059. [21] Esat et al. (1978) *GRL, 9*, 807. [22] Fahey et al. (1987) *GCA, 51*, 329. [23] McKeegan et al. (2005) *LPS, 36*, #2077. [24] Yurimoto et al. (2005) in *Protostars & Planets V*, 845. [25] Fujii et al. (2006) *EPSL, 247*, 1. [26] Berquist & Blum (2007) *Science, 318*, 417. [27] Manhes & Göpel (2007) *GCA, 71*, A618. Supported by NASA grant NNX07AI81G (ANK) and NAG5-11591 (Klaus Keil).

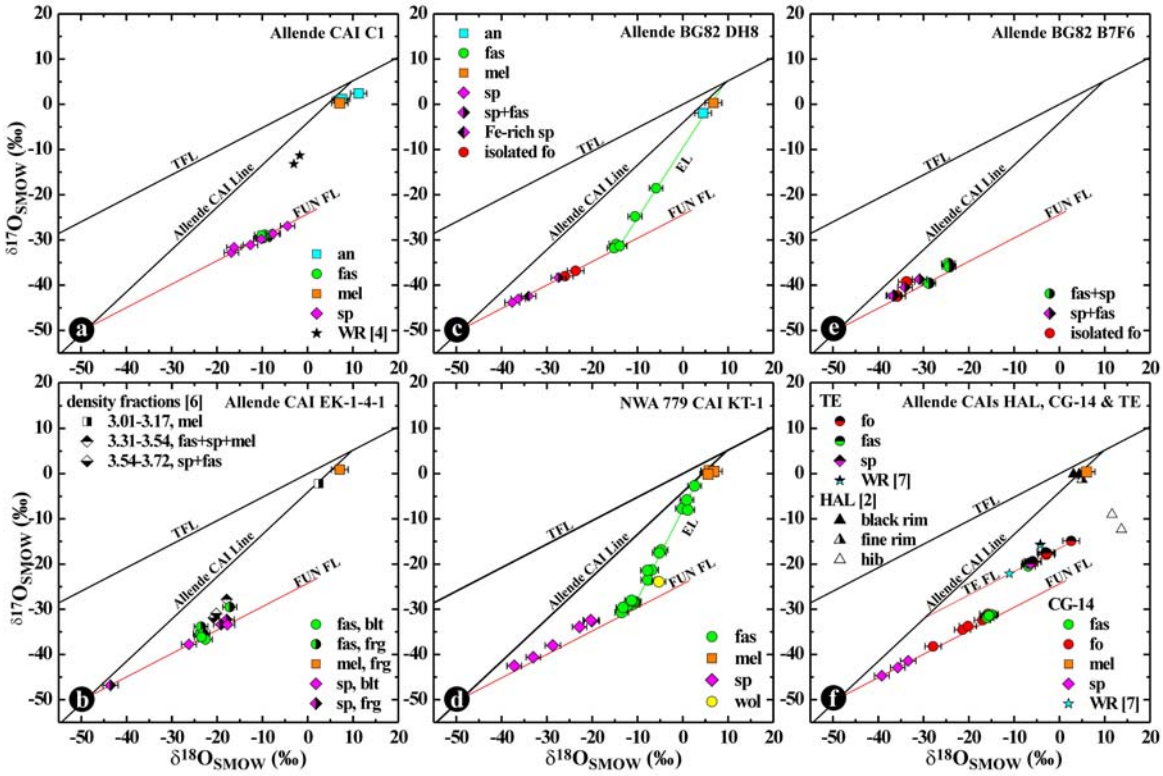

Fig. 1. Oxygen isotopic compositions of the Allende FUN CAIs C1, EK 1-4-1, BG82 DH8, BG82 B7F6, CG14, HAL, the NWA 779 FUN CAI KT-1 [data from 13], and the Allende F CAI TE. TFL = terrestrial fractionation line; FUN FL = FUN fractionation line defined by the data for spinel and fassaite from C1; EL = exchange lines defined by the data for fassaite in B7F6 and KT-1. O-isotopic compositions of individual minerals from FUN CAIs define mass-dependent fractionation line with $\Delta^{17}O \sim -24‰$. The degree of fractionation among spinel (sp), fassaite (fas) and forsterite (fo) is generally consistent with their inferred crystallization sequence: sp → sp+fo → sp+fo+fas; melilite and anorthite are ^{16}O-depleted, suggesting postcrystallization isotopic exchange. Some of the fassaite grains in DH8 and KT-1 show evidence for subsequent isotopic exchange with an ^{16}O-poor reservoir, probably during partial melting of the host CAIs. Oxygen isotopic compositions of fassaite, spinel and forsterite in sample TE define their own mass-fractionation line parallel to the Fun FL but intersecting the CAI line at a much higher point ($\Delta^{17}O \sim -17‰$). This and other observations [10-12] suggest a multistage formation history for this CAI, Shown are 2σ errors for $\delta^{18}O$; 2σ errors for $\delta^{17}O$ correspond to size of the symbols.